Chapter 3

Modeling of the Two-Way Shape Memory Effect

Meddour Belkacem and Brek Samir

Additional information is available at the end of the chapter

http://dx.doi.org/10.5772/intechopen.75657

Abstract

The shape memory alloys (SMA) are distinguished from other conventional materials by a singular behavior which takes many forms depending on the thermomechanical load. The two-way shape memory effect is one of these forms. The interest that exhibits this behavior is that the material can remember two states, so this leads to many industrial applications. This thermoelastic property is driven by the temperature under residual stress of education. To model this effect in 3D, we considered stress and temperature as control variables and the fraction of martensite as internal variable; choosing Gibbs free energy expression and applying thermodynamic principles with transformation criteria have permitted to write the constitutive equations that control this behavior. The constructed model is then numerically simulated, and finally, the proposed model appears applicable in engineering.

Keywords: two-way, simulation, hysteresis, transformation

1. Introduction

Shape memory alloys (SMA) as they are called are a kind of particular materials which have a singular behavior, they can be largely deformed (about 10%) under an applied mechanical, a simple heating is sufficient to recover the previous form, that is why they are called that way.

By varying controlled parameters (stress and temperature), these alloys can exhibit other properties like pseudoelasticity, two-way shape memory effect, one-way shape memory effect [1, 2], and reorientation effect [3].

These properties derive from phase transformations, i.e., higher temperature phase (austenite) to lower temperature phase (martensite).

It is observed that these phase transformations do not occur with diffusion but rather with displacement, i.e., displacement at a distance less than interatomic [4, 5].

These important properties made them requested materials in various fields such as biomedical automotive industry, fire watch devices, aeronautics, and medical devices [6].

Two-way shape memory effect is obtained after the alloy is subjected to an education [7], i.e., to a cyclic thermal load under a constant mechanical load (**Figure 1**).

It should be noted that the previous education is performed to create a field of internal stresses, which will substitute the macroscopic ones; under a cyclic thermal load, the alloy will remember two states: one is at lower temperature (martensite) and the other at higher temperature (austenite) (**Figure 2**).

The next steps in this paper are to build the constitutive model and simulate it using an algorithm; regarding model parameters, we will use the work of [8].

2. Methods and materials

2.1. Constitutive equations

Let us choose the following free energy expression:

$$G(\sigma = \sigma_{00}, T, f) = -\sigma_{00} : S_A : \sigma_{00} - f.\varepsilon_0.\sigma_{00} : R + f.B.\left(T - M_s^0\right) + C.f.(1 - f) \qquad (1)$$

S_A: Fourth order tensor of complaisance; B, C: Constants to be determined, respectively, related to change of phase and interaction between austenite and martensite; f: Fraction of martensite; $\boldsymbol{\sigma_{00}}$: Tensor of stress created after education.

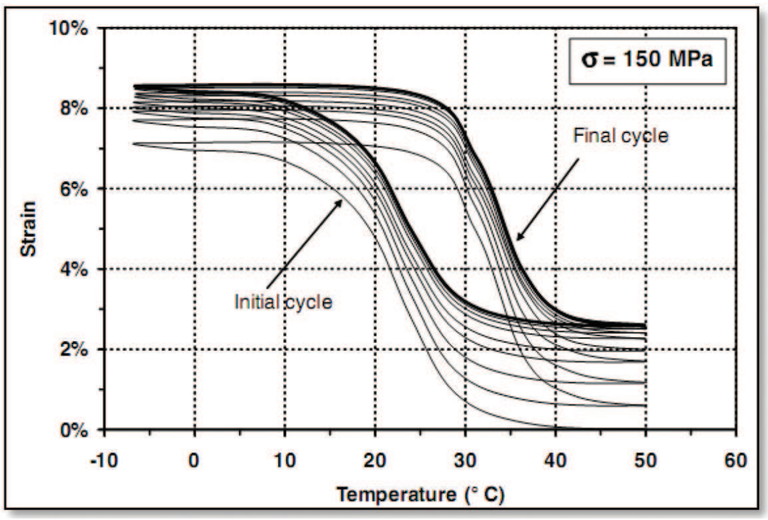

Figure 1. Education (50 cycles) performed on a NiTi wire under constant stress of 150 MPa [7].

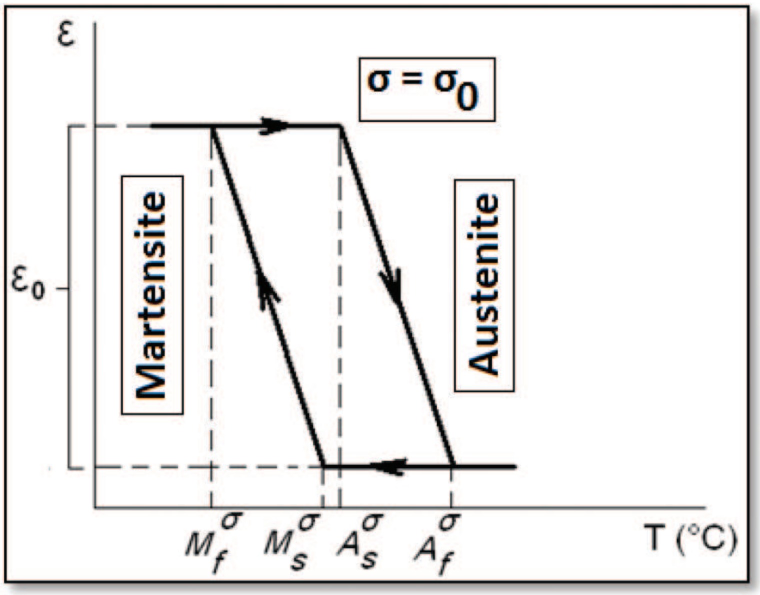

Figure 2. One-dimensional two-way effect. M_s^σ : Temperature of transformation start A- > M under stress σ.M_f^σ : Temperature of transformation finish A- > M under stress σ.A_s^σ : Temperature of transformation start M- > A under stress σ. A_f^σ : Temperature of transformation finish M- > A under stress σ. ε_0: Uniaxial maximum deformation.

Assuming that dissipation is associated only with transformation (fraction of martensite) [9, 10], the second principle of thermodynamics can be written as

$$-\frac{\partial G}{\partial f}.\frac{df}{dt}\geq 0 \tag{2}$$

Let us write the driving force F^{th}:

$$F^{th}=-\frac{\partial G}{\partial f} \tag{3}$$

Then,

$$F^{th}=\varepsilon_0.\sigma_{00}:R-B.\left(T-M_s^0\right)+C(2f-1) \tag{4}$$

Because of hysteresis, there is a dissipative force F^{di}, which will oppose F^{th}.

We choose expression of F^{di}:

$$F^{di}=Kf+H \tag{5}$$

Transformation occurs when

$$F^{th}=F^{di} \tag{6}$$

We introduce the criteria functions:

$$\varphi^{di} = F^{th} - F^{di}; \dot{f} > 0; f \geq 0 \ ; \ f \leq 1 \tag{7}$$

$$\varphi^{di}(\sigma = \sigma_{00}, T, f) = \varepsilon_0.\sigma_{00} : R - B.(T - M_s^0) + C(2f - 1) - Kf - H \tag{8}$$

Condition of consistence gives

$$d\varphi^{di}(\sigma = \sigma_{00}, T, f) = 0; \dot{f} > 0; f \geq 0 \ ; f \leq 1 \tag{9}$$

$$\frac{\partial \varphi^{di}}{\partial \sigma} d\sigma + \frac{\partial \varphi^{di}}{\partial T} dT + \frac{\partial \varphi^{di}}{\partial f} df = 0 \ (d\sigma = 0) \tag{10}$$

$$df = \frac{B.dT}{(2C - K)}; \dot{f} > 0 \tag{11}$$

Doing the same with the reverse transformation

$$\varphi^{in}(\sigma = \sigma_{00}, T, f) = \varepsilon_0.\sigma_{00} : R - B.(T - M_s^0) + C(2f - 1) + Gf + H \tag{12}$$

$$df = \frac{B.dT}{(2C + K)}; \dot{f} < 0; f \geq 0 \ ; f \leq 1 \tag{13}$$

Eqs. (11) and (13) give the evolution of fraction of martensite.

The deformation resulting from transformation of austenite to martensite is denoted $\boldsymbol{\varepsilon}^T$; this deformation is associated with fraction of martensite:

$$d\varepsilon^T = df.\varepsilon_0.R; \dot{f} > 0; f \geq 0 \ ; f \leq 1 \tag{14}$$

R is a tensor of transformation, and it can be written as the following:

$$R = \frac{\sigma}{\sqrt{\sigma:\sigma}} \tag{15}$$

$$d\varepsilon^T = \frac{B.dT}{(2C - K)} \varepsilon_0.R; \dot{f} > 0; f \geq 0 \ ; f \leq 1 \tag{16}$$

$$d\varepsilon^T = \frac{B.dT}{(2C + K)} \varepsilon_0.R; \dot{f} < 0; f \geq 0 \ ; f \leq 1 \tag{17}$$

2.2. Determination of constants *B*, *C*, *K*, and *H*

At the beginning of direct transformation

$$\sigma_{00} = \begin{pmatrix} \sigma_0 & 0 & 0 \\ 0 & 0 & 0 \\ 0 & 0 & 0 \end{pmatrix}, T = M_s^\sigma, f = 0 \tag{18}$$

$$\varphi^{di}(\sigma = \sigma_{00}, T = M_s^\sigma, f = 0) = \varepsilon_0.\sigma_{00} : R - B.(M_s^\sigma - M_s^0) + C - H = 0 \tag{19}$$

At the end of the direct transformation

$$\sigma_{00} = \begin{pmatrix} \sigma_0 & 0 & 0 \\ 0 & 0 & 0 \\ 0 & 0 & 0 \end{pmatrix}, T = M_f^\sigma, f = 1 \tag{20}$$

$$\varphi^{di}\left(\sigma = \sigma_0, T = M_f^\sigma, f = 1\right) = \varepsilon_0.\sigma_0 : R - B.\left(M_f^\sigma - M_s^0\right) - C - K - H = 0 \tag{21}$$

At the beginning of the reverse transformation

$$\sigma_{00} = \begin{pmatrix} \sigma_0 & 0 & 0 \\ 0 & 0 & 0 \\ 0 & 0 & 0 \end{pmatrix}, T = A_s^\sigma, f = 1 \tag{22}$$

$$\varphi^{in}\left(\sigma = \sigma_0, T = A_s^\sigma, f = 1\right) = \varepsilon_0.\sigma_0 : R - B.\left(A_s^\sigma - M_s^0\right) - C + K + H = 0 \tag{23}$$

At the end of the reverse transformation

$$\sigma_{00} = \begin{pmatrix} \sigma_0 & 0 & 0 \\ 0 & 0 & 0 \\ 0 & 0 & 0 \end{pmatrix}, T = A_f^\sigma, f = 0 \tag{24}$$

$$\varphi^{in}\left(\sigma = \sigma_0, T = A_f^\sigma, f = 0\right) = \varepsilon_0.\sigma_0 : R - B.\left(A_f^\sigma - M_s^0\right) + C + H = 0 \tag{25}$$

2.3. Experimental data

Table 1 illustrates experimental data and material constants *B*, *C*, *K*, and *H*. The used material is CuZnAl. The test was performed under constant stress ($\sigma = 65$ MPa).

2.4. Numerical simulation

2.4.1. One-dimensional case

We considered a segment of CuZnAl submitted to a constant stress ($\sigma = 65$ MPa) and a thermal load ($300 \leq T \leq 400$ K) (**Figure 3**).

$M_s^0(K)$	**313**	$M_s^\sigma(K)$	**324**	E_A(**MPa**)	**72,000**
$M_f^0(K)$	303	$M_f^\sigma(K)$	311	E_M(**MPa**)	70,000
$A_s^0(K)$	315	$A_s^\sigma(K)$	330	ε_0	0.023937
$A_f^0(K)$	325	$A_f^\sigma(K)$	340	*H*(MPa)	0.2606751918
B(MPa.K^1)	3.258439*E*-2	*C*(MPa)	0.18736036121	*K*(MPa)	4.8876464*E*-2
υ	0.3				

Table 1. Experimental data [8, 11].

2.4.2. Three-dimensional case

The considered specimen is a cubic element subjected to a constant mechanical load which is a triaxial traction and thermal loads ($\sigma_{11} = \sigma_{22} = \sigma_{33} = 50$ MPa) and ($300 \leq T \leq 400$ K) (**Figures 4–6**).

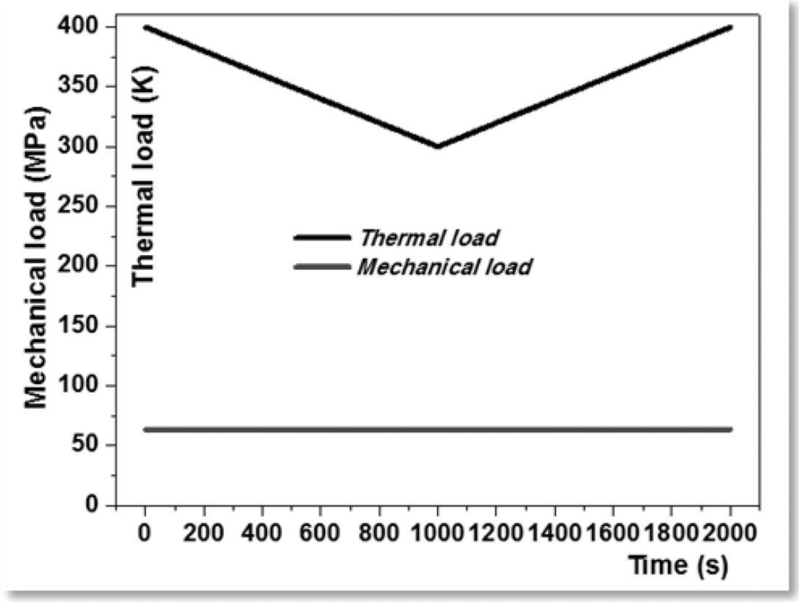

Figure 3. History of coupled loading.

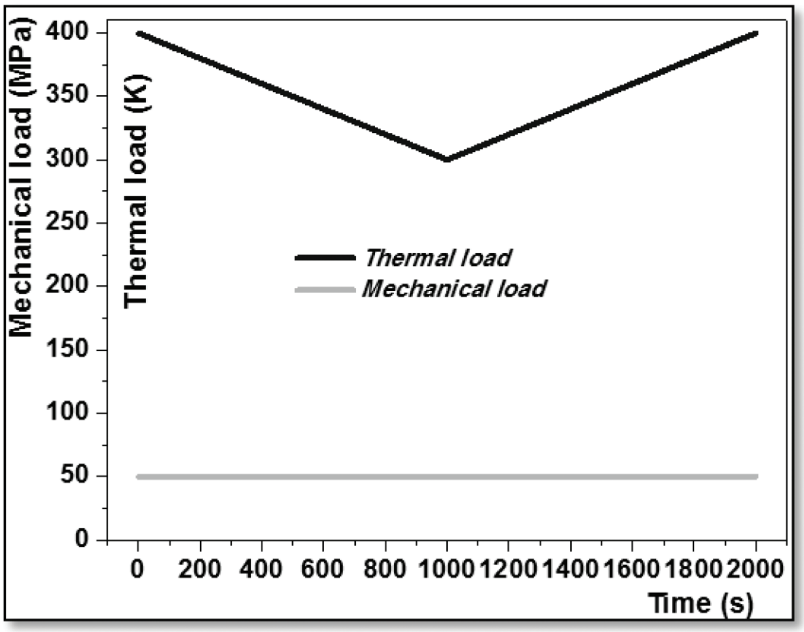

Figure 4. Loading in the direction of σ_{11}.

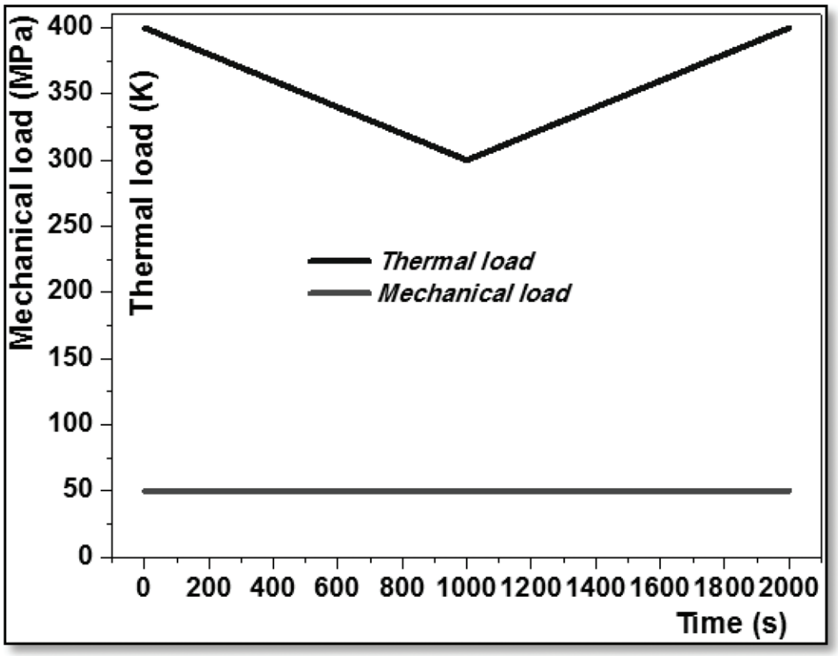

Figure 5. Loading in the direction of σ_{22}.

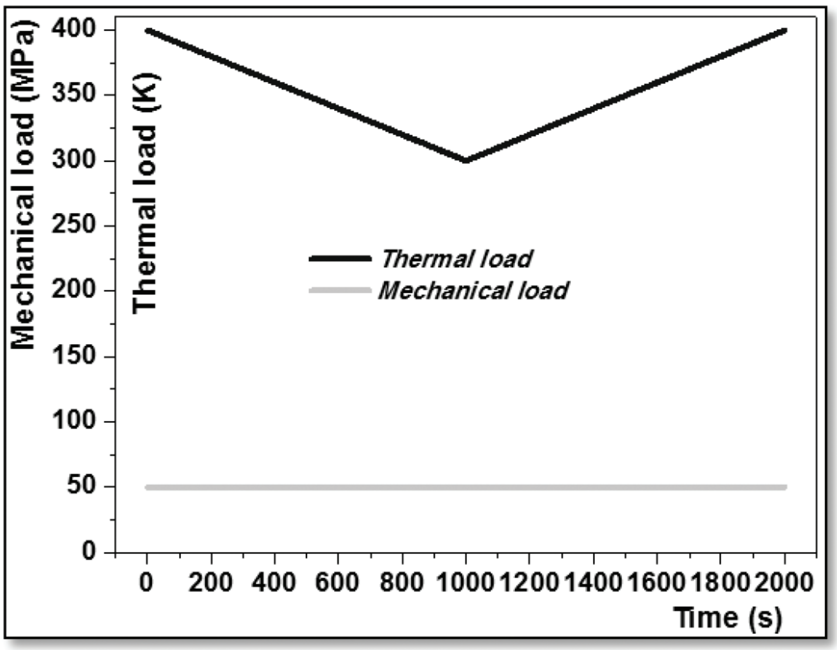

Figure 6. Loading in the direction of σ_{33}.

3. Results

3.1. One-dimensional case

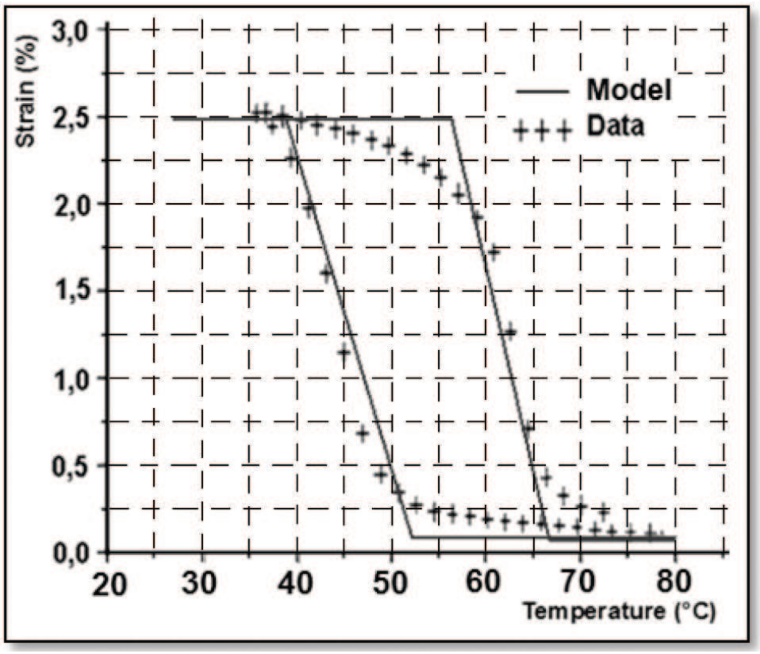

Figure 7. Response at (σ = **65 MPa**).

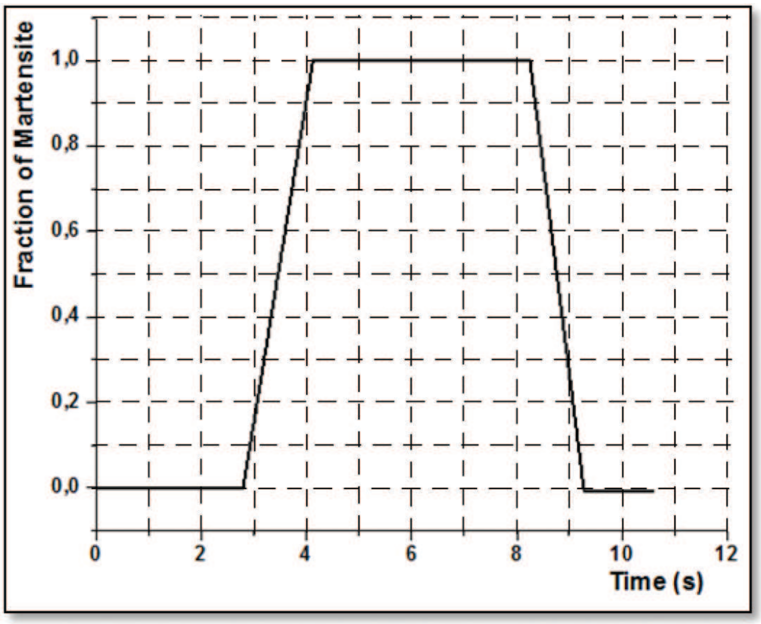

Figure 8. Evolution of the fraction of martensite.

http://dx.doi.org/10.5772/intechopen.75657

3.2. Three-dimensional case

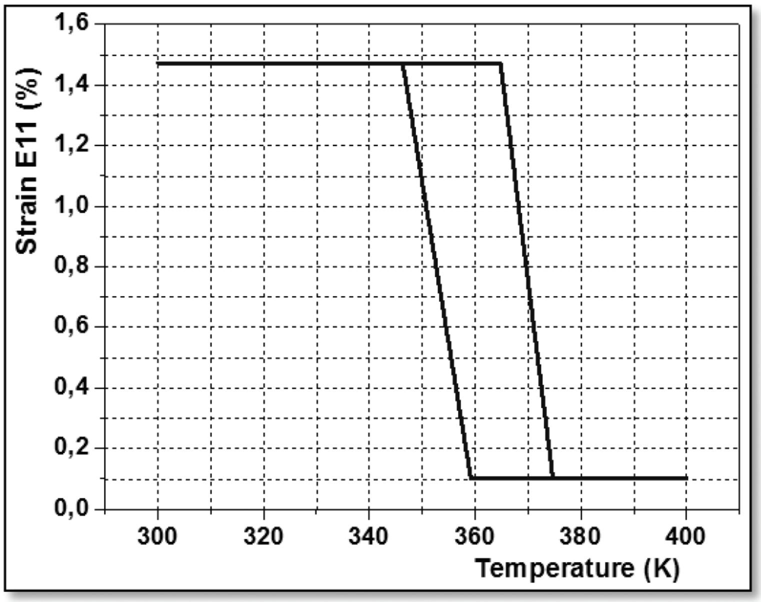

Figure 9. Plot $T-\varepsilon_{11}$.

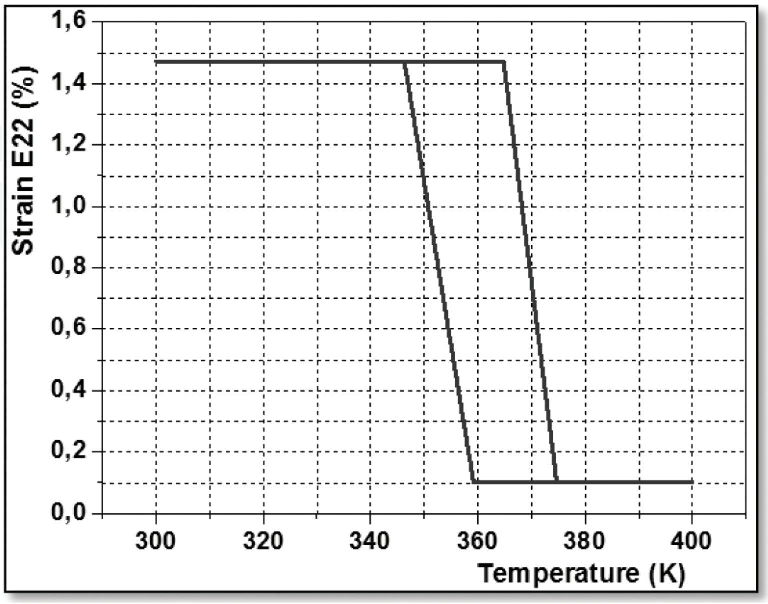

Figure 10. Plot $T-\varepsilon_{22}$.

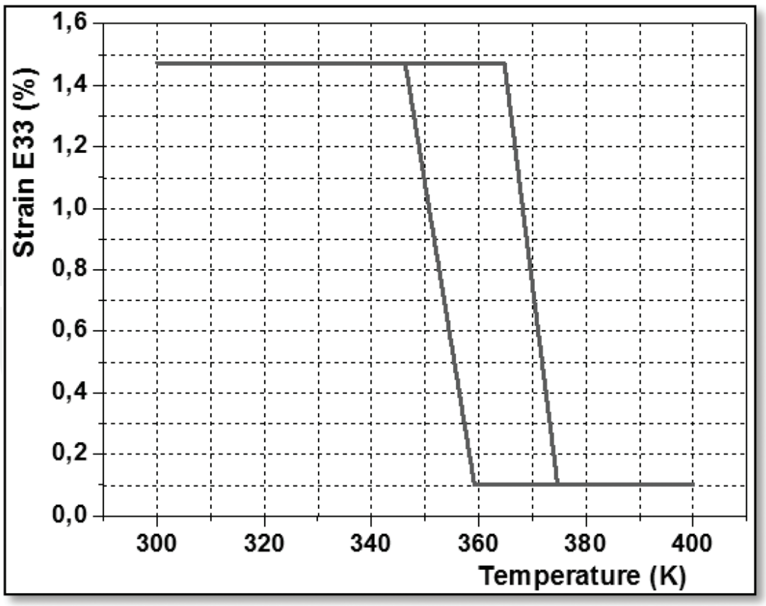

Figure 11. Plot $T - \varepsilon_{22}$.

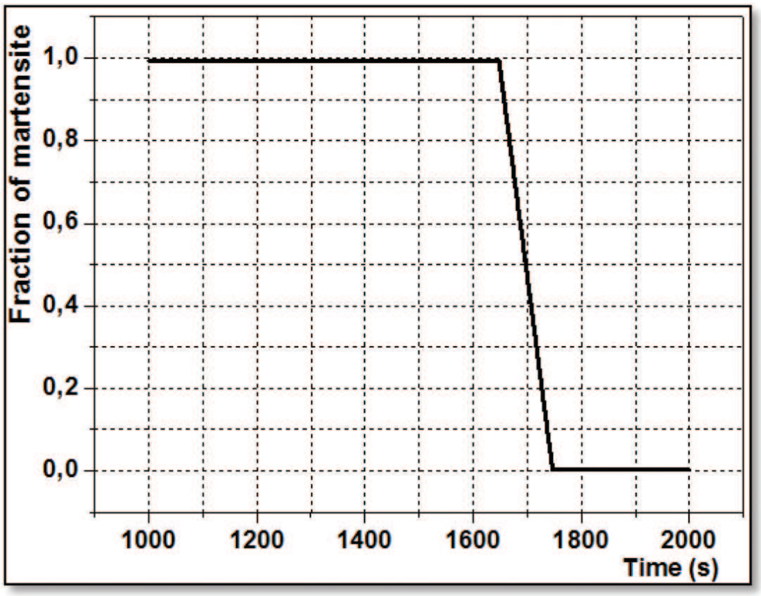

Figure 12. Evolution of fraction of martensite in direct transformation.

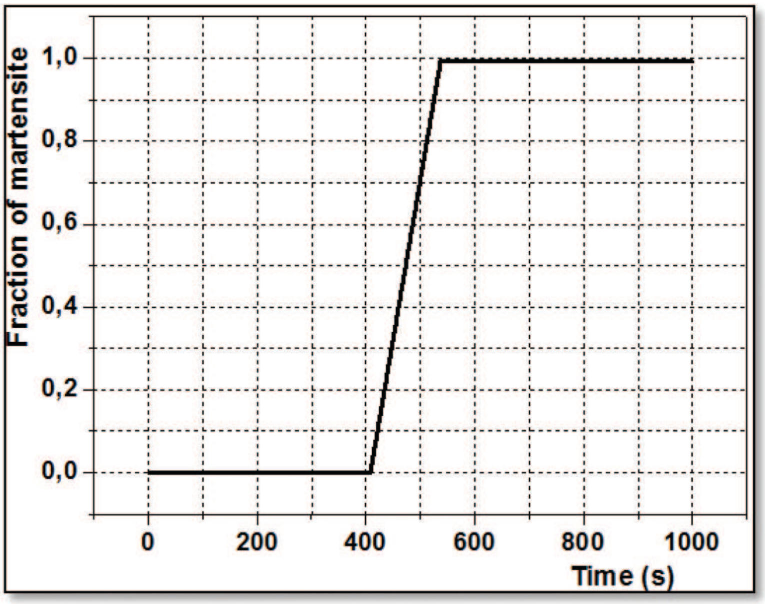

Figure 13. Evolution of fraction of martensite in reverse transformation.

4. Discussion

After having written constitutive equations and criteria functions, the numerical simulation has permitted to obtain previous results.

First, we used the extracted values from the curve of the test in order to compare this curve with the response of the model in one-dimensional case, and we obtained **Figure 7**. This figure presents a good agreement between experimental data and the model response.

On the other hand, **Figure 8**, which is representing the evolution of the martensite fraction, is also in agreement with the curve in **Figure 7**, i.e., the direct transformation and the reverse transformation are functions of martensite fraction. We can say that the constitutive model behaves well in one-dimensional case.

For the three-dimensional case, **Figures 9–11** show the response under the triaxial traction and thermal load; for each plot, there is a hysteresis.

The shrinking of the hysteresis in each case of the figures should be noted (**Figures 9–11**); this is due to the triaxial loading.

Despite the applied triaxial load, **Figures 9–11** exhibit the thermomechanical cycle as it is in case of one-dimensional two-way effect (**Figure 7**).

Figures 12 and **13** show the evolution of fraction of martensite for each case of direct and reverse transformations, and the shapes of the plots are compatible with **Figures 9–11** as the one-dimensional case because it was noticed previously that the deformation is proportional to the amount of martensite.

5. Conclusion

In this work, we have developed a 3D constitutive model using the principles of thermodynamics and a simple formalism, and these principles have permitted to write criteria of transformation. This macroscopic model is developed by simple formalism and assumptions.

By using an algorithm, we have implemented the model, and the response seems to be compatible with the nature of the two-way shape memory effect. In the one-dimensional case, we have observed a good agreement between the numerical and experimental plots.

It should be noted that the parameters of the model were determined by the one-dimensional test and further used in the biaxial and triaxial cases to ensure consistency of the model in different cases of loading. The implementation of the model in the algorithm is simple and practical. The obtained results testify the usability of the developed model.

At the end, we can say that this macroscopic constitutive model can be used in applications to engineering problems, in order to particularly simulate the pseudoelastic effect of shape memory alloys.

Author details

Meddour Belkacem* and Brek Samir

*Address all correspondence to: samsum66@gmail.com.in

Department of Mechanical Engineering, University of Khenchela, Algeria

References

[1] Arghavani J, Auricchio F, Naghdabadi R, Reali A, Sohrabpour S. A 3D phenomenological constitutive model for shape memory alloys under multiaxial loadings. International Journal of Plasticity. 2010;**26**:976-991

[2] Yutaka T, Jong-Bin L, Minoru T. Finite element analysis of superelastic, large deformation behaviour of shape memory alloy helical springs. Computers and Structures. 2004;**82**: 1685-1693

[3] Pan H, Thamburaja P, Chau FS. Multi-axial behaviour of shape memory alloys undergoing martensitic reorientation and detwinning. International Journal of Plasticity. 2007;**23**: 711-732

[4] Otsuka K. Perspective of research on martensitic transformations present and future. Journal de Physique IV. 2001;**11**:3-9

[5] J. Van Humbeeck. La transformation martensitique, dans Technologie des. Chapter 3. In: Alliages ’a M’emoire de Forme. Paris, France: Hermes; 1993. pp. 63-88

[6] Duerig T, Pelton A, Stockel D. An overview of nitinol medical applications. Materials Science and Engineering. 1999;**A273-275**:149-160

[7] Miller DA, Lagoudas DC. Thermo-mechanical characterization of NiTiCu and NiTi SMA actuators: Influence of plastic strains. Smart Materials and Structures. 2000;**9**(5):640-652

[8] Bourbon G, Lexcellent C, Leclercq S. Modelling of the non-isothermal cyclic behaviour of a polycrystalline Cu-Zn-Al shape memory alloy. Journal de Physique IV. 1995;**5**(C8):221-226

[9] Patoor E, Eberhardt A, Berveiller M. On Micromechanics of Thermoelastic Phase Transition. The proceedings of Plasticity 93: The Fourth International Symposium on Plasticity and Its Applications, Baltimore, Maryland. 1993, July. 19-23

[10] Lagoudas DC, Entchev PB. Modeling of transformation-induced plasticity and its effect on the behavior of porous shape memory alloys. Part I: Constitutive model for fully dense SMAs. Mechanics of Materials. 2004;**36**(9):865-892

[11] Shape Memory Applications Inc. Available from: http://heim.ifi.uio.no/~mes/inf1400/COOL/Robot%20Prosjekt/Flexinol/Shape%20Memory%20Alloys.htm